Asian Journal of Advanced Research and Reports

16(11): 25-36, 2022; Article no.AJARR.92056
ISSN: 2582-3248

Tropospheric Influence on Low-band Very High Frequency (VHF) Radio Waves

Ukoette Jeremiah Ekah [a*], Emmanuel Obi [a] and Igwe Ewona [a]

[a] Department of Physics, Cross River University of Technology, Calabar, Nigeria.

Authors' contributions

This work was carried out in collaboration among all authors. All authors read and approved the final manuscript.

Article Information

DOI: 10.9734/AJARR/2022/v16i11436

Open Peer Review History:
This journal follows the Advanced Open Peer Review policy. Identity of the Reviewers, Editor(s) and additional Reviewers, peer review comments, different versions of the manuscript, comments of the editors, etc are available here: https://www.sdiarticle5.com/review-history/92056

Original Research Article

Received 18 July 2022
Accepted 22 September 2022
Published 10 October 2022

ABSTRACT

The objectives of this study are to understudy the effects of temperature and relative humidity on low-band VHF signals, obtain a propagation model for signal transmission over Calabar and to ascertain the suitability of the free space propagation model for the study terrain. Results obtained shows that temperature and relative humidity has no effect on low-band VHF signals. The suitability of the free space propagation model for the study terrain failed, as calculated results underestimated path losses in the study area. Multiple regression analysis was used to obtain a suitable propagation model for the study terrain. However, since the studied meteorological variables has no effect on low-band VHF signals in the study area, the measured path losses could be attributed to foliage, hills, distance away from the transmitter and other components of the study terrain in which the signal is propagated.

Keywords: VHF signals; radio waves; temperature; relative humidity; path loss.

1. INTRODUCTION

The International Telecommunication Union (ITU) designation for the range of radio frequency electromagnetic waves, from 30 to 300 megahertz (MHz), with corresponding wavelength of ten meters to one meter is called the Very High Frequency (VHF) radio waves. They propagate mainly by line-of-sight and are blocked by obstacles. However, due to refraction, they travel beyond the visual horizon to about 160 km [1,2].

VHF radio waves are used for FM radio broadcast, two-way land mobile radio systems, long-range data communication, marine

**Corresponding author: Email: ukoettejeremiah@crutech.edu.ng;*

communications, etc. There are two VHF bands, the low-band VHF (49-108 MHz) and high-band VHF (169-216 MHz). Low-band VHF radio waves of 49 MHz is used for transmission of wireless microphones, cordless phones, radio-controlled toys and more. Slightly higher VHF radio waves of 54-72 MHz operates television channels 2-4, as well as wireless systems. VHF radio waves of 76-88 MHz operate television channels 5 and 6. The highest low band VHF is 88-108 MHz which is used for the commercial FM radio broadcast band [3].

The basis of the radio communication system is the electromagnetic wave theory. There are a variety of phenomena that occur when an electromagnetic wave is incident on a surface. These phenomena depend upon the polarization of the wave, the geometry of the surface, the material properties of the surface and the characteristics of the surface relative to the wavelength of the electromagnetic wave. As electromagnetic waves propagate through the earth's atmosphere, they carry information over long distances without wires. However, they are affected by the medium in which there are propagating and as such, results to a reduction in signal power at the receiver's end [2-4].

In communication systems, radio waves radiate from an antenna and travel outward in all directions. It is affected by the environment depending on its range of frequency and may travel to the receiving antenna by various modes of wave propagation [4,5]. As they travel, signal strength of radio waves radiating from the transmitter to the receiver are affected by atmospheric conditions even at line-of-sight situations. These atmospheric variables causes the propagated waves to vary from its anticipated range. The higher the frequency, the higher its chances of being distorted by tropospheric variables [6]. This weakens the received signal, as some of its energies are reflected, refracted, absorbed, depolarized, scattered and diffracted [7-27].

Studies have been carried out by several researchers to explore the effect of atmospheric elements on radio waves [28-36], but the results and conclusions have been contradictory. Some research studies claim that relative humidity is the main factor while others claim that temperature is the dominating factor [37-40].

For instance, in [30], though the authors did not state the transmitting frequency, however, they mentioned that the research was investigating signals in the VHF band. Obtained result depicts that path loss increases as temperature increases while path loss reduces as relative humidity increases. This implies that as temperature increases, signal strength reduces and as relative humidity increases, received signal strength increases. The authors in [34,38] investigated signals in the low-band VHF range. The results were contradicting. While [34] concluded that temperature increase reduces path loss, the result was the reverse for the authors in [38]. Also, while [34] concluded that an increase in relative humidity led to an increase in path loss, the result was the opposite for the authors in [38]. In [39], the authors investigated high-band VHF radio waves and came with the conclusions that an increase in temperature reduces path loss and vice versa, while an increase in relative humidity increases path loss and vice versa.

Sequel to the need for a proper understanding of the effects of temperature and relative humidity on low-band VHF radio waves in order to ease its deployment for signal transmission in any terrain, this paper aims at determining how temperature and relative humidity affects signals in the VHF low-band using signals generated from a transmitter at a frequency of 105.5MHz. The obtained result will be used to develop a propagation model for the study area and make comparison with the existing free space propagation model. This is done to check the suitability of the free space propagation model for transmission of signal in the study area.

1.1 Free Space Propagation Model

This involves loss in signal strength in decibels (dB), as signals travel from the transmitter to the receiver. It is calculated by discounting hindrances that occur in its transmission path. For a sphere with radius d and surface area A,

$$A = 4\pi d^2 \tag{1}$$

At a distance d, away from the transmitter, the power per unit area

$$P_{Di} = \frac{P_T}{4\pi d^2} \tag{2}$$

Practically, all antennas provide directional propagation, hence, directivity gain

$$G_T = \frac{P_D}{P_{Di}} \tag{3}$$

where P_D = power density along mean axis of radiation antenna radiation and P_{Di} = power density of an isotropic antenna. From (3),

$$P_D = G_T P_{Di} \quad (4)$$

Putting (2) into (4)

$$P_D = \frac{P_T G_T}{4\pi d^2} \quad (5)$$

At the receiving end, let P_R be the power received at the receiving antenna. Under matched conditions and effective aperture of antenna at maximum directivity A_e

$$P_R = P_D A_e \quad (6)$$

But,

$$A_e = \frac{G_R \lambda^2}{4\pi} \quad (7)$$

Where λ is the wavelength of the radiated wave and G_R is the maximum directivity gain of the antenna

Putting (7) into (6)

$$P_R = \frac{P_D G_R \lambda^2}{4\pi} \quad (8)$$

Putting (5) into (8)

$$P_R = \frac{P_T G_T G_R \lambda^2}{16\pi^2 d^2} \quad (9)$$

Therefore,

$$\frac{P_R}{P_T} = \frac{G_T G_R \lambda^2}{(4\pi d)^2} \quad (10)$$

But,

$$V = f\lambda \quad (11)$$

Therefore,

$$\lambda = \frac{V}{f} \quad (12)$$

Where V is the speed of light and f is the transmission frequency
putting (12) into (10)

$$\frac{P_R}{P_T} = \frac{G_T G_R V^2}{(4\pi f d)^2} \quad (13)$$

Substituting V = 3.0 × 10^8 m/s and $\pi = \frac{22}{7}$ into (13)

We have,

$$\frac{P_R}{P_T} = 0.0005 \frac{G_T G_R}{(fd)^2} \quad (14)$$

Converting (14) to decibel (dB), we have

$$\left(\frac{P_R}{P_T}\right)_{(dB)} = G_T + G_R - (32.5 + 20 \log d + 20 \log f) \quad (15)$$

Putting $P_{L\ (dB)}$ for $\left(\frac{P_R}{P_T}\right)_{(dB)}$

$$P_{L\ (dB)} = G_T + G_R - (32.5 + 20 \log d + 20 \log f) \quad (16)$$

Equation 16 is the free space transmission equation in decibel (dB). In a summary,

$$P_{L\ (dB)} = G_T + G_R - L_{FS} \quad (17)$$

Where,

$$L_{FS} = 32.5 + 20 \log d + 20 \log f \quad (18)$$

Where f is in megahertz (MHz) while d is in kilometers (Km)

2. METHODOLOGY

2.1 Equipment Used for Data Collection

A digital spectrum analyzer (GW-INSTEK) GSP-730 with frequency range of 150 MHz - 3GHz was used in measuring the signal strength while a digital thermometer and hygrometer (model Htc) was used in measuring temperature and relative humidity. A hand-held GPS (GARMIN 78S) was used for the measurement of latitude and longitude. This work was carried out in the city of Calabar, Cross River State. Measurements of received signal strength, geographical coordinates (elevation, longitude and latitude) and meteorological variables were simultaneously taken. Measurement were taken in twelve locations, based on the peculiarity of the location.

2.2 Data Collection

Signals transmitted from the base station of Cross River Broadcasting Corporation at a frequency of 105.5MHz was measured at Line-of-Sight (LOS) distance at 12 different routes

with the base station as the reference point. The received signal strengths were obtained at the receiver antenna at a height of 3.0 m. During the measurement campaign, elevation, latitude and longitude at the various points of data collection were measured using the GPS. Concurrently, temperature and relative humidity was measured.

2.3 Data Analysis

Measured data was grouped according to routes and the average values were used for the analysis. The data for received signal strength, temperature and relative humidity were averaged for each location. Line of Sight (LOS) distance of each measurement point was calculated, taking the base station as the reference point. Path loss of the measured signal was calculated as

$$P_L = P_T - P_R \quad (19)$$

Where,

P_T = Transmitted power
P_R = Received power
P_L = Loss in power

Where P_T = 68.451dBm

Various graphs were plotted and the correlation coefficients between the measured path loss and temperature/relative humidity was calculated for a proper understanding of the effects of temperature and relative humidity on low-band VHF signals. A path loss model to suit with the terrain of the study area was obtained using multiple regression analysis. Finally, free space path loss was calculated using the free space path loss equation and the calculated values were compared with the measured path loss model. This was done to ascertain its suitability for transmission of low-band VHF signals in the study terrain. Where the free space path loss model does not suit with the terrain, an optimized free space path loss model was developed.

3. RESULTS AND DISCUSSION

3.1 Effects of Temperature and Relative Humidity on VHF Radio Waves

Table 1 contains the average temperature, average relative humidity and the measured path loss obtained from equation (19).

From the data in Table 1, graphs of measured path loss against temperature and relative humidity have been plotted as shown in Figs. 1 and 2, with correlation coefficients of 0.09 and 0.14 obtained for measured path loss against temperature and measured path loss against relative humidity, respectively. The values of the correlation coefficientsimply that temperature and relative humidity has insignificant effects on low-band VHF signals. Hence, this result does agree with earlier results obtained [30,34,38,39].

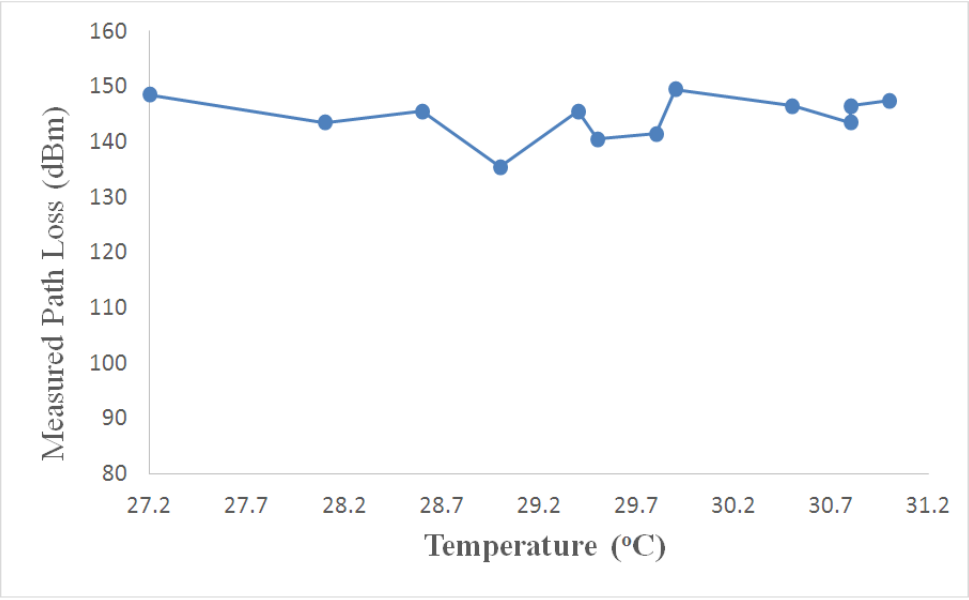

Fig. 1. Graph of Measured Path loss against Temperature

Table 1. Averages of temperature, relative humidity and measured Path loss

Location	Temperature (^oC)	Relative Humidity (%)	Measured Path Loss (dBm)
A	28.1	69	143.451
B	27.2	68	148.451
C	29.5	61	140.451
D	29.9	61	149.451
E	30.5	60	146.451
F	30.8	59	146.451
G	28.6	66	145.451
H	29.8	58	141.451
I	30.8	70	143.451
J	29.0	60	135.451
K	31.0	61	147.451
L	29.4	59	145.451

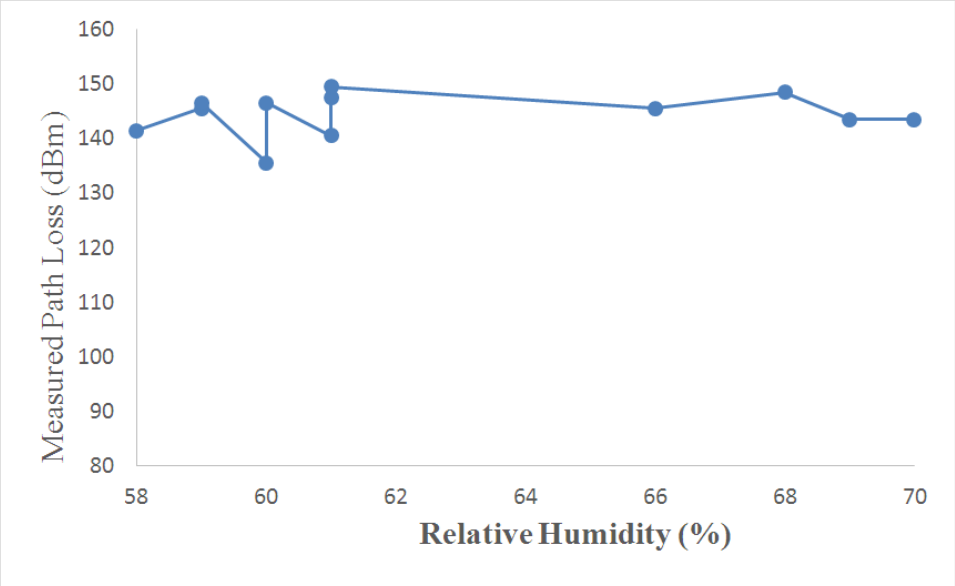

Fig. 2. Graph of measured path loss against relative humidity

3.2 Path Loss Model for Study Area using Multiple Regression Analysis

Multiple regression analysis was used in developing a path loss model for the study area. In this model, path loss was considered the dependent variable while temperature and relative humidity were the independent variables. This was done based on the assumption that temperature and relative humidity influenced signal transmission between the transmitter and the receiver. In multiple regression analysis,

$$Y = \beta_o + \beta_1 T + \beta_2 R + \mu \quad (20)$$

Where

Y = P = calculated path loss
β_o = constant
β_1= predictor variable for temperature
β_2= predictor variable for relative humidity
μ = prediction error
T = temperature
R= relative humidity

Here,

β_o = 112.720
β_1= 0.639
β_2= 0.205
μ = 3.648

Therefore, regression model becomes

$$P = 112.720 + 0.639T + 0.205R + 3.648 \quad (21)$$

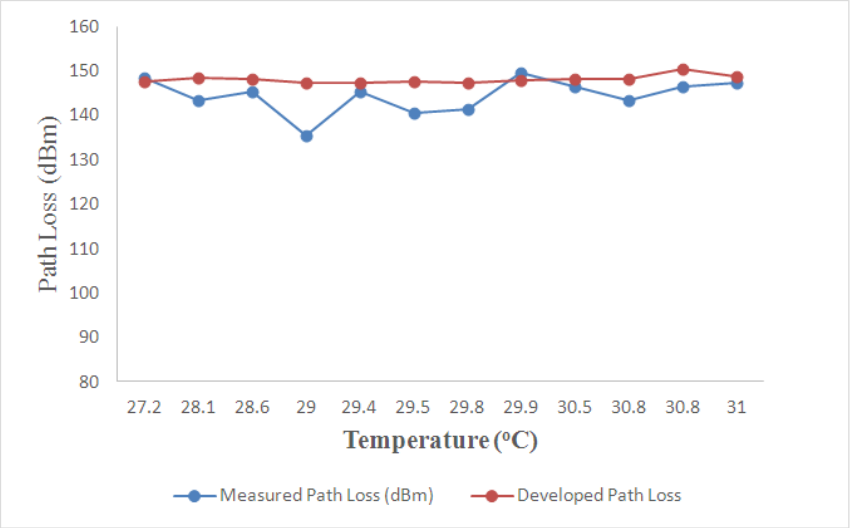

Fig. 3. Graph of Measured Path loss/Developed Path Loss against Temperature

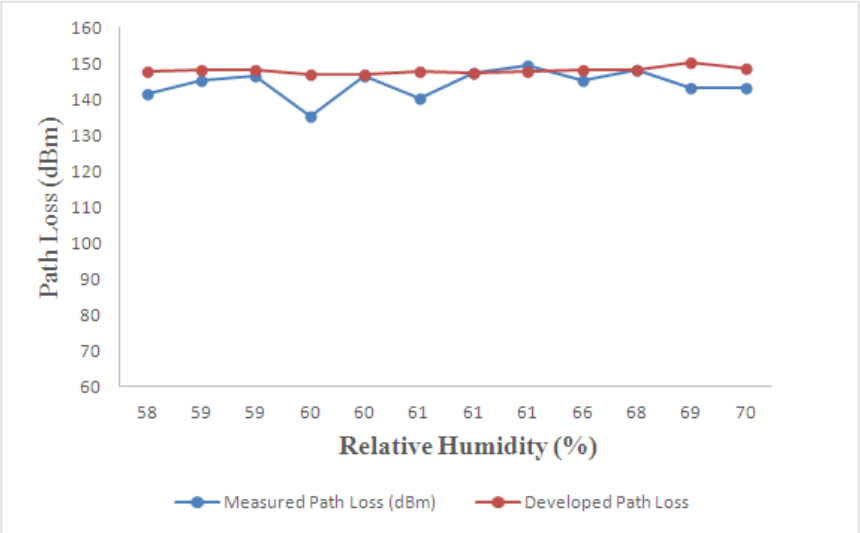

Fig. 4. Graph of measured path loss / developed path loss against relative humidity

Table 2. Calculated LOS distance of measurement location from base station

Location	LOS Distance (Km)
A	14.700
B	18.219
C	16.919
D	14.548
E	12.679
F	7.902
G	0.394
H	5.172
I	6.895
J	11.227
K	12.359
L	11.865

Equation (21) becomes the path loss model in the study area. This means that a unit increase in temperature results to 0.639dBm increase in path loss and a unit increase in relative humidity results to 0.205dBm increase in path loss. The low prediction error of 3.648dBm indicates a better fit for the model. The average values of temperature and relative humidity were inserted into equation (21) and the obtained path losses were plotted against temperature/relative humidity, as shown in Figs. 3 and 4.

3.3 Analysis of Free Space Propagation Model

From the longitudes and latitudes of the measured routes and that of the base station as the reference point, the LOS distance of each location from the base station was obtained. This is presented in Table 2.

From Table 2, loss in signal propagation for the free space model is determined. Recall, path loss for free space propagation is given in equation (18) as

L_{FS} = 32.5 + 20 log d + 20 log f

Hence, in location A, LOS distance = 14.700km

L_{FS} = 32.5 + 20 log 14.700 + 20 log 105.5 = $96.311dBm$

In location B, LOS distance = 18.219km,

L_{FS} = 32.5 + 20 log 18.219 + 20 log 105.5 = $98.176dBm$

In location C, LOS distance = 16.919km,

L_{FS} = 32.5 + 20 log 16.919 + 20 log 105.5 = $97.553dBm$

In location D, LOS distance = 14.548km,

L_{FS} = 32.5 + 20 log 14.548+ 20 log 105.5 = $96.221dBm$

In location E, LOS distance = 12.679km,

L_{FS} = 32.5 + 20 log 12.679+ 20 log 105.5 = $95.027dBm$

In location F, LOS distance = 7.902km,

L_{FS} = 32.5 + 20 log 7.902 + 20 log 105.5 = $90.920dBm$

In location G, LOS distance = 0.394km,

L_{FS} = 32.5 + 20 log 0.394 + 20 log 105.5 = $64.875dBm$

In location H, LOS distance = 5.172km,

L_{FS} = 32.5 + 20 log 5.172 + 20 log 105.5 = $87.238dBm$

In location I, LOS distance = 6.895km,

L_{FS} = 32.5 + 20 log 6.895 + 20 log 105.5 = $89.736dBm$

In location J, LOS distance = 11.227km,

L_{FS} = 32.5 + 20 log 11.227 + 20 log 105.5 = $93.970dBm$

In location K, LOS distance = 12.359km,

L_{FS} = 32.5 + 20 log 12.359 + 20 log 105.5 = $94.805dBm$

In location L, LOS distance = 11.865km,

L_{FS} = 32.5 + 20 log 11.865 + 20 log 105.5 = $94.450dBm$

From Table 3, Figs. 5 and 6, a wide difference in the measured and calculated path losses is observed. The free space path loss model underestimates the actual path loss in the terrain. This shows that the free path loss model is not a suitable propagation model for signal transmission in the study area. Hence, an adjustment of the free space propagation model for its suitability for signal transmission in the study area must be implemented.

3.4 Optimization of Free Space Propagation Model

Recall, in equation (18), free space path loss model is given as

L_{FS} = 32.5 + 20 log d + 20 log f

To optimize the model for its suitability in the study area, we introduce a prediction error C. Therefore,

$$L_{FS} = 32.5 + 20 \log d + 20 \log f + C \qquad (22)$$

And

$$C = \sqrt[2]{\frac{(P_m - P_{FS})^2}{N}} \qquad (23)$$

Where C = 53.7dBm

Therefore,

$$L_{FS} = 32.5 + 20 \log d + 20 \log f + 53.7 \quad (24)$$

From equation (24), the optimized free space path losses for each location is obtained as shown in Table 4. Also, graphs of measured path loss/optimized free space path loss against temperature/relative humidity are plotted in Figs. 7 and 8.

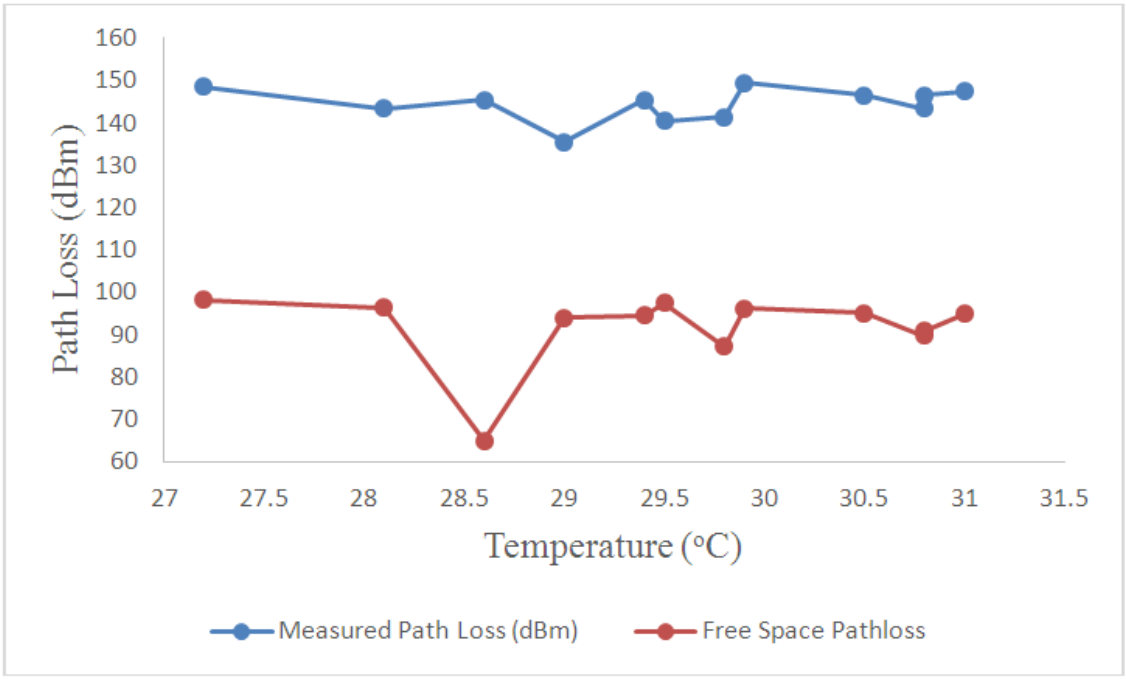

Fig. 5. Graph of measured / free space path loss against temperature

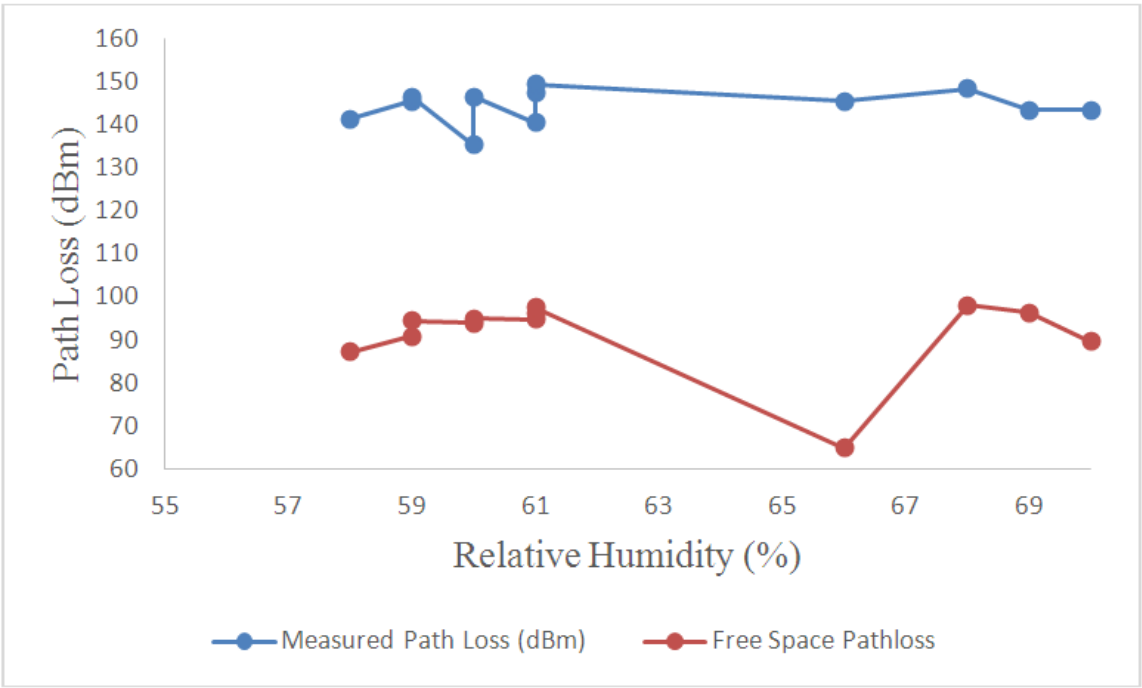

Fig. 6. Graph of measured/free space path loss against relative humidity

Table 3. Average temperature and relative humidity / Measured and free space path losses

Location	Temperature (°C)	Relative Humidity (%)	Measured Path Loss (dBm)	Free Space Loss (dBm)
A	28.1	69	143.451	96.311
B	27.2	68	148.451	98.176
C	29.5	61	140.451	97.533
D	29.9	61	149.451	96.221
E	30.5	60	146.451	95.027
F	30.8	59	146.451	90.920
G	28.6	66	145.451	64.875
H	29.8	58	141.451	87.238
I	30.8	70	143.451	89.736
J	29.0	60	135.451	93.970
K	31.0	61	147.451	94.805
L	29.4	59	145.451	94.450

Table 4. Average temperature and relative humidity / Measured and free space path losses

Location	Temperature (°C)	Relative Humidity (%)	Measured Path Loss (dBm)	Optimized Free Space Loss (dBm)
A	28.1	69	143.451	150.011
B	27.2	68	148.451	151.876
C	29.5	61	140.451	151.233
D	29.9	61	149.451	149.921
E	30.5	60	146.451	148.727
F	30.8	59	146.451	144.620
G	28.6	66	145.451	118.875
H	29.8	58	141.451	140.938
I	30.8	70	143.451	143.436
J	29.0	60	135.451	147.670
K	31.0	61	147.451	148.505
L	29.4	59	145.451	148.150

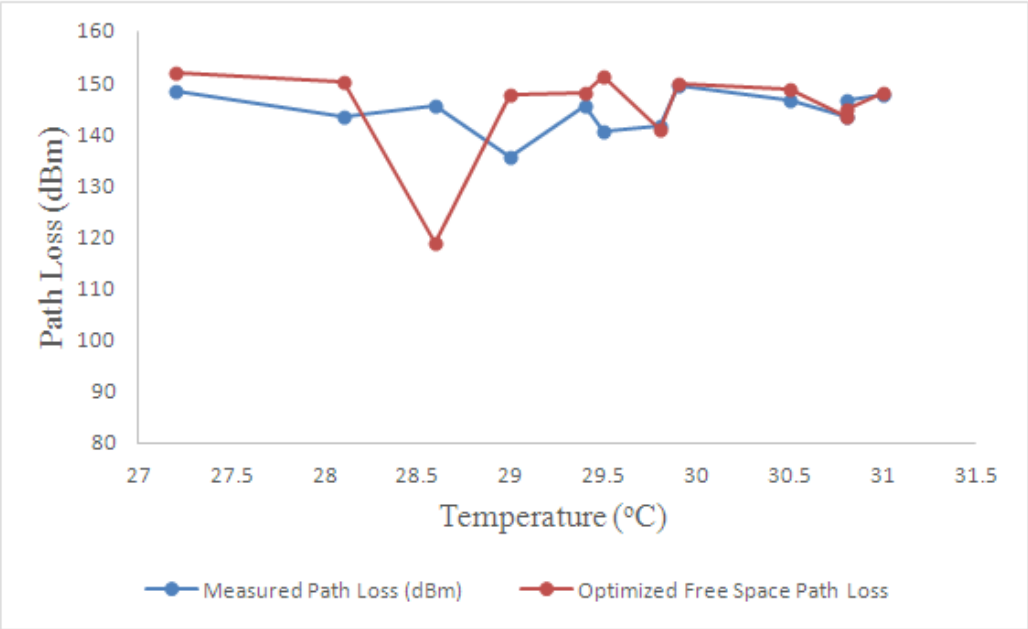

Fig. 7. Graph of measured / optimized free space path loss against temperature

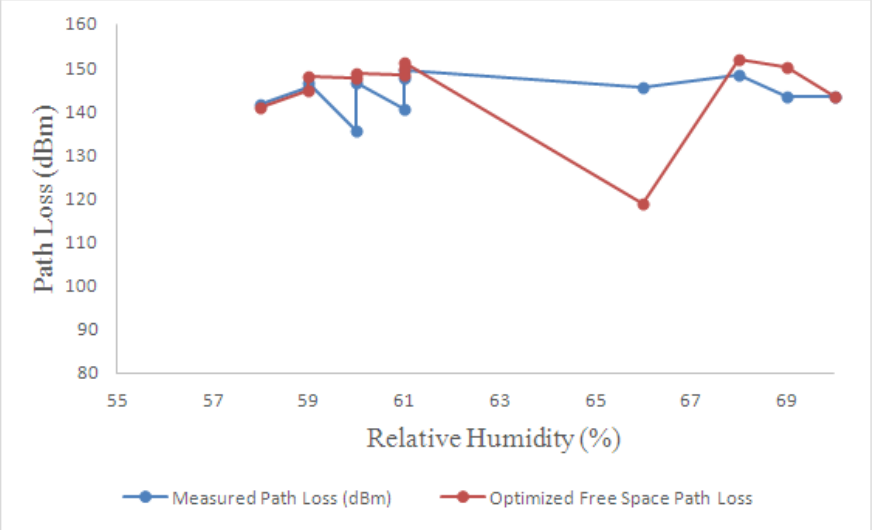

Fig. 8. Graph of measured / optimized free space path loss against relative humidity

Since the prediction error is above the recommended threshold of at most 6dBm [41], it is justifiable to say that the optimized free space path loss model is not fit for signal propagation in the area under investigation. This is not unconnected to the overestimation and underestimation of path losses, as observed in Figs. 7 and 8.

4. CONCLUSION

The effects of meteorological variables on low-band VHF signals have been studied, taking temperature and relative humidity as the meteorological variables of importance. Results obtained shows that temperature and relative humidity has no effect on VHF signals. The suitability of the free space propagation model for the study terrain failed, as calculated results showed that this model underestimated path losses in the study area. Multiple regression analysis has been used to obtain a suitable path loss model for the study terrain. However, we recommend further research to be carried out in this study region, the check the effects of distance, hills, foliage and other environmental parameters on low-band VHF signals in the study area.

ACKNOWLEDGEMENT

The authors of this article are thankful to the Tertiary Education Trust Fund (TETFund), Nigeria, for the grant support that enabled the undertaking of this research.

COMPETING INTERESTS

Authors have declared that no competing interests exist.

REFERENCES

1. Rec. ITU-R V.431-8, Nomenclature of the frequency and wavelength bands used in telecommunications; 2021. Available:https://www.itu.int/dms_pubrec/itu-r/rec/v/R-REC-V.431-8-201508-I!!PDF-E.pdf [retrieved Dec 31, 2021].
2. Seybold JS. Introduction to RF propagation. New York: John Wiley & Sons, Inc; 2005. 349 p.
3. Ekah UJ, Adebayo AO, Shogo OE. Spatial distribution of frequency modulated signals in Uyo, Nigeria. World J Adv Eng Technol Sci. 2022;5(1):39-46.
4. Raj A. Wireless communications. 1st Ed. Delhi: Khanna Publishers; 2014.
5. Baker DN, Erickson PJ, Fennell JF, Foster JC, Jaynes AN, Verronen PT. Space weather effects in the Earth's radiation belts. Space Sci Rev. 2018;214(1):1-60.
6. Isabona J, Imoize AL, Rawat P, Jamal SS, Pant B, Ojo S et al. Realistic prognostic modeling of specific attenuation due to rain at microwave frequency for tropical climate region. Wirel Commun Mob Comput. 2022;2022:1-10.
7. Ekah UJ, Onuu MU. Tropospheric influence on call setup in mobile networks. J Eng Res Rep. 2022;22(2):14-26.

8. Akinbolati A, Ajewole MO. Effect of some radio climatic factors on digital terrestrial television signal in a Sahel savannah city of Nigeria. Fudma J Sci. 2020;4(2):111-8.
9. Kale R. Impact of weather and climate on Internet connection. International Journal of Research Publication and Reviews. 2021;2(11):212-6.
10. Onuu MU, Umoh E, Nwosu CN. Rain attenuation of radio waves in South-Eastern Nigeria. Adv Appl Sci. 2022;7(1):15-20.
11. Ekah BJ, Iloke J, Ekah UJ. Tropospheric influence on dropped calls. Glob J Eng Technol Adv. 2022;10(2):83-93.
12. Mmahi NO, Akinbolati A, Ikechiamaka FN, Akpaneno FA, Joseph E, Ekundayo KR. Studies on surface radio refractivity over some selected cities in North-Central, Nigeria. Fudma J Sci. 2021;5(4):90-9.
13. Nemah HA, Ahmed MM, Khaleed OL, Nemat GS. Effect of some meteorological variables and conditions on mobile phone and TV satellite signal. Transport. 2020;32(2):71-5.
14. Isabona J, Imoize AL, Ojo S, Lee CC, Li CT. Atmospheric propagation modelling for terrestrial radio frequency communication links in a tropical wet and dry savanna climate. Information. 2022 Mar 7;13(3):1-16.
15. Akpan CS, Onuu MU. Design and construction of a weather instrument and its use in measurements to determine the effects of some weather parameters on GSM signal strength. Adv Appl Sci. 2021;6(4):142-54.
16. Ewona I, Ekah U. Influence of tropospheric variables on signal strengths of mobile networks in Calabar, Nigeria. J Sci Eng Res. 2021;8(9):137-45.
17. Ekah UJ, Iloke J, Ewona I, Obi E. Measurement and performance analysis of signal-to-interference ratio in wireless networks. Asian J Adv Res Rep. 2022;16(3):22-31.
18. Emeruwa C, Ekah UJ. Pathloss model evaluation for long term evolution in Owerri. Int J Innov Sci Res Technol. 2018;3(11):491-6.
19. Emeruwa C, Ekah UJ. Investigation of the Variability of Signal strength of Wireless Services in Umuahia, Eastern Nigeria. IOSR JAP. 2018;10(3):11-7.
20. Ewona I, Ekah UJ, Ikoi AO, Obi E. Measurement and performance assessment of GSM networks using received signal level. J Contemp Res. 2022;1(1):88-98.
21. Iloke J, Utoda R, Ekah U. Evaluation of radio wave propagation through foliage in parts of Calabar, Nigeria. Int J Sci Eng Res. 2018;9(11):244-9.
22. Ekah UJ, Iloke J. Performance evaluation of UMTS key performance indicators in Calabar, Nigeria. GSC J Adv Res Rev. 2022;10(1):47-52.
23. Tamošiūnaitė M, Žilinskas M, Tamošiūnienė M, Tamošiūnas S. Atmospheric attenuation due to humidity. Electromagn Waves. 2011 Jun 21;157.
24. Ekah UJ, Emeruwa C. Guaging of key performance indicators for 2G mobile networks in Calabar, Nigeria. World J Adv Res Rev. 2021;12(2):157-63.
25. Obi E, Ekah U, Ewona I. Real-time assessment of cellular network signal strengths in Calabar. Int J Eng Sci Res Technol. 2021;10(7):47-57.
26. Ekah UJ, Emeruwa C. A comparative assessment of GSM & UMTS networks. World J Adv Res Rev. 2022;13(1):187-96.
27. Lim NC, Yong L, Su HT, Chai AY, Vithanawasam CK, Then YL et al. Review of temperature and humidity impacts on RF signals. In 2020 13th International UNIMAS Eng Conference (EnCon). IEEE Publications; 2020 Oct 27. p. 1-8.
28. Usman I, Ibrahim MN, Akeem LS, Shehu A. Effects of radio-climatic variables on signal propagation in Kebbi State. Caliphate J Sci Technol. 2020;2(1): 18-24.
29. Chima AI, Onyia A, Udegbe SU. The effects of atmospheric temperature and wind speed on UHF radio signal; a case study of ESUT community and its environs in Enugu State. IOSR JAP. 2018;10(2): 83-90.
30. Suleman KO, Bello IT, Tijani LO, Ogunbode AO, Olayiwola WA. Effect of temperature and ground water on VHF radio wave propagation in tropical climate. Int J Sci Eng Res. 2017;8(1):1391-6.
31. Mat R, Shafie MM, Ahmad S, Umar R, Seok YB, Sabri NH. Temperature effect on the tropospheric radio signal strength for UHF band at Terengganu, Malaysia. International Journal on Advanced Science, Engineering and Information Technology. 2016;6(5):770-4.
32. Mat R, Sabri NH, Umar R, Ahmad S, Zafar SNAS, Omar A et al. Effect of humidity on tropospheric Received Signal Strength

(RSS) in Ultra-High Frequency (UHF) band. J Phys Conf S. 2020; 1529(042048).
33. Mat R, Hazmin SN, Umar R, Ahmad S, Zafar SN, Marhamah MS. The modelling of tropical weather effects on ultrahigh frequency (UHF) radio signals using SmartPLS. InIOP Conference Series. Mater Sci Eng. 2018;440(1):012041.
34. Alade MO. Investigation of the effect of ground and air temperature on very high frequency radio signals. J Inf Eng Appl. 2013;3(9):16-21.
35. Ukhurebor KE. Influence of meteorological variables on UHF radio signal: recent findings for EBS, Benin City, South-South, Nigeria. Discovery. 2018;54(269): 157-63.
36. Alade MO. Dry Hot and Cool Tropical Climate Attenuation models at VHF. Int J Electron Commun Comput Eng. 2013;4(4):1114-8.
37. Luomala J, Hakala I. Effects of temperature and humidity on radio signal strength in outdoor wireless sensor networks. In2015 Fed Conference on Computer Science and Information Systems (FedCSIS). IEEE Publications; 2015;1247-55.
38. Felix A, Ayegba A, Paul J, Joshua A. Assessment of the Effect of Atmospheric Pressure on the signal strength of frequency modulation radio station-WE FM Abuja Nigeria. 2018;8(6): 141-6,
39. Ukhurebor KE, Olayinka SA, Nwankwo W, Alhasan C. Evaluation of the effects of some weather variables on UHF and VHF receivers within Benin City, South-South region of Nigeria. J Phys Conf S. 2019;1299(1):012052.
40. Rao SN, Babu LK, Parthasarathy V. Effect of environmental parameters on long range wi-fi connectivity. In 2017 8th International Conference on Computing, Communication and Networking Technologies (ICCCNT). IEEE Publications; 2017;1-6.
41. Olatoye NO, Ekoko EC, Sani OM, Ogungbenro O. The Determination of Pathloss Model for Ultra-High-Frequency television Transmission in Onitsha, Anambra state, Nigeria. Int J Commun Syst. 2021;34(5):e4716.

Peer-review history:
The peer review history for this paper can be accessed here:
https://www.sdiarticle5.com/review-history/92056